



Gold nanoparticles-coated polystyrene beads for the multiplex detection of viral DNA



Hassan H. Fakh, Malek M. Itani, Pierre Karam*

The Department of Chemistry, American University of Beirut, P.O. Box 11-0236, Beirut, Lebanon

ARTICLE INFO

Article history:

Received 15 November 2016

Received in revised form 7 April 2017

Accepted 11 April 2017

Available online 15 April 2017

Keywords:

Multiplex detection

Flow cytometry

Polystyrene beads

Hepatitis B virus

Vaccinia virus

ABSTRACT

We report on the preparation of a sensing platform for the fast multiplex detection of short oligonucleotide sequences. Monodispersed micro-sized polystyrene beads (average diameter of ca. 4.72 μm) were prepared and subsequently coated with nanosized gold nanoparticles. The micro-sized beads are large enough to scatter light and allow the detection of specific analytes using flow cytometry. Fluorescently labeled DNA hairpins are assembled onto the gold nanoparticles. In the absence of the target sequence, the metal particles quench the probe signal. Upon hybridization, the fluorescent signal of the hairpin is turned on and is readily detected by the flow cytometer with a detection limit of 5 nM. The sensing platform was able to sense and discriminate in parallel two specific genetic markers of Vaccinia virus and hepatitis B virus. Viral sequences spiked in an artificial serum were readily detected with comparable sensitivity to the buffer solution. The assay time was optimized from the assembly to testing to take less than 2 h including a hybridization of 30 min.

© 2017 Elsevier B.V. All rights reserved.

1. Introduction

Specific and sensitive oligonucleotide sensors are growing to be revolutionary tools for prognosis, diagnosis and treatment of genetic and infectious diseases [1–7]. Their importance stems from the fact, for instance, that some cancerous cells and viral diseases spread by communicating their genetic information via blood circulating oligonucleotide strands [8,9]. MicroRNA is an example of these small non-coding oligonucleotides (22nt) [10,11]. In addition, statistically unique short sequences that are complementary to specific viruses and bacteria have also been identified and been exploited in many sensing schemes for rapid identification of infectious diseases [12,13]. The sensing of the circulating or unique oligonucleotides translates into early disease diagnosis which in general correlates with the recovery and survival rate from these diseases [14].

Over the past few years, an increasing number of methods had emerged to detect short oligonucleotide sequences based on quantitative real-time polymerase chain reaction [15–17], in situ hybridization [18–20] and high throughput sequencing [21,22]. These methods are however expensive and in situ hybridization is technically challenging and semi-quantitative. Other more

recent biosensing schemes were designed specifically to reduce the assay complexity and time span. Kelley et al. have designed an electrochemical method based on nanostructured microelectrodes capable of detecting short DNA sequences with low detection limits in the attomolar range and a fast assay time (ca. 30 min) [23–25]. Mirkin et al. have also reported a highly selective and sensitive method based on quenching/recovery of fluorescent signals which extended the detection of specific oligonucleotide sequences to the cellular cytoplasm [13,26].

Despite these tremendous advances, the field of oligonucleotide sensing still lacks abundance in methods with multiplexing capabilities [27–29]. Biological systems are complex which makes diagnosis based on the detection of a single analyte prone to high false positives and negatives. The multiplex detection of specific markers that are either closely related or directly correlated leads to the increase in the level of accuracy in diagnosis and reduces, considerably, the materials and time. For instance, six specific miRNA biomarkers are over expressed in prostate cancer patients [30], another five in gastric cancer [31], and eleven in lung cancer [32]. The parallel detection of these specific biomarkers, for instance, will be a great step forward for the early diagnosis of cancer. Hence improving the alacrity, simplicity and specificity of multiplex-based platforms is an ongoing challenge in the biosensing field [33].

In this work, we report a multiplex platform for the detection of oligonucleotides that complies simplicity and specificity

* Corresponding author.

E-mail address: pierre.karam@aub.edu.lb (P. Karam).

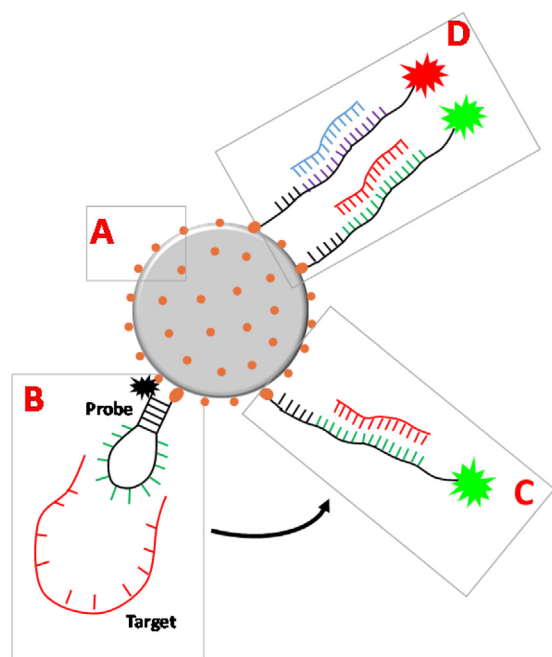


Fig. 1. Schematic representation of the operational scheme of the sensing platform divided into four major phases. (A) Phase 1: Synthesis of monodispersed polystyrene beads coated with gold nanoparticles. (B) Phase 2: Assembly of fluorescently labeled DNA hairpin onto the gold nanoparticles. The folded oligonucleotide brings the fluorescent dye in close proximity to the metal surface leading to its quenching. (C) Phase 3: detection of specific oligonucleotide targets. Upon hybridization the fluorescent dye signal is recovered due to the induced unfolding of the hairpin. The fluorescent signal is detected using flow cytometry. (D) Phase 4: Multiplex detection of two or more targets is possible by modifying the DNA hairpin with spectrally resolved fluorescent dyes.

in its operational scheme. The probe is based on a fluorescently labeled DNA hairpin (molecular beacon) complementary to a specific target and immobilized on gold nanoparticles decorating micro-sized polystyrene beads. In the absence of the target, the folded oligonucleotide will bring the fluorophore in close proximity to the gold nanoparticle surface (Fig. 1B) [34]. The dye will be completely quenched. Upon hybridization to a complementary target, the hairpin will open up and the fluorescent signal is restored (Fig. 1C) [35,36]. To achieve multiplexing capabilities and low detection limits, flow cytometric measurements were employed. The polystyrene beads, each decorated with multiple probes, single file through the laser path and trigger the detection of the target of interest [37]. The sensing platform could be easily modified to detect any sequence of interest.

2. Reagents and materials

Styrene monomer, polyvinylpyrrolidone powder (PVP, MW 55K), gold(III) chloride trihydrate ($\text{AuCl}_3 \cdot 3\text{H}_2\text{O}$), sodium citrate, potassium phosphate mono and dibasic (KH_2PO_4 , K_2HPO_4), dithiothreitol (DTT) and 2-methoxyethanol were all purchased from Sigma–Aldrich. 4,4'-Azobis (4-cyanovaleric acid) (ACVA) was purchased from Bide Pharmatech. The phosphate buffer (PBS) was prepared using the mono and dibasic phosphate at final concentration of 0.01 M and pH = 7.

Short oligonucleotides hairpin and target sequences were obtained from Integrated DNA Technologies IDT (Table 1). Deionized water and all buffers used in the experiments were filtered through 0.22 μm membranes before use.

Table 1

Specific oligonucleotide sequences for hepatitis B virus (HBV) and Vaccinia virus (VV) used in this study.

HBV-Target	5'-TTG GCT TTC AGT TAT ATG GAT GAT GTG GTA-3'
HBV-Probe	5'-Thiol-C6/ GTT GGT ACC ACA TCA TCC ATA TAA CTG AAA GCC AAC/ ATTO488-3'
VV-Target	5'-AGT TGT AAC GGA AGA TGC AAT AGT AAT CAG-3'
VV-Probe	5'-Thiol-C6/ GGA GTT CTG ATT ACT ATT GCA TCT TCC GTT ACA ACT CC/ ATTO647N-3'

3. Methods

3.1. Gold coated polystyrene beads (PS-Au)

Micro-sized and monodispersed PS beads were synthesized by dispersion polymerization as previously described [38–40]. Briefly, 0.5 g of PVP and 0.1 g of ACVA were dissolved in a solvent mixture of methoxyethanol (15.5 mL), ethanol (6.5 mL) and water (2.0 mL) (Fig. 2A). The solution was deoxygenated by purging it with nitrogen for 15 min. Upon addition of 20 mL of styrene, the mixture is heated to 70 °C and kept under constant stirring at 80 rpm for 24 h. The obtained beads are centrifuged and washed three times with deionized water at 800 rpm to obtain homogenous micro-beads. In a subsequent step, the beads are decorated with gold nanoparticles [41]. One milliliter of the previously prepared beads is washed in a 1:0.5 ethanol–water solution to remove excess PVP and ensure the nucleation of gold nanoparticles on the particle surface. To a boiling solution of Au^{3+} (100 mL; 5.5×10^{-4} H AuCl_4), the washed PS is added followed by sodium citrate, at a final concentration of 8×10^{-2} M. PS gold decorated beads were centrifuged four times to separate any unbound gold nanoparticles and resuspended in deionized water.

3.2. DNA hairpin assembled onto PS-Au particles

The assembly of the hairpin sequences on the gold coated polystyrene beads was achieved following a modified reported salting procedure [42]. Initially, DNA hairpins are suspended in a PBS (0.01 M, pH = 7.01) at a final concentration of 10^{-4} M. DTT (0.1 M) is then added to the solution to break any disulfide bonds. A microspin G-25 column is used to isolate the free DNA strands. A desired concentration of hairpins is added to the previously prepared PS-Au solution. Incremental amounts of NaCl is added to the assembly every 15 min for an hour to reach a final concentration of 0.6 M. Unbound hairpins are removed by centrifuging the solution at 900 rpm for 8–9 min.

3.3. Oligonucleotide sensing

PS gold decorated beads modified with fluorescently labeled DNA hairpins are suspended in a hybridization buffer consistent of 5 mM Tris–HCl, 1 mM ethylenediaminetetraacetic acid (EDTA), and 0.5 M NaCl, pH = 7.01 [43]. DNA target sequences of specific concentrations are incubated with the micro-beads assembly for 30 min, unless otherwise stated. For the detection of bound targets of interest, the sample was analyzed using flow cytometry (SORP Aria II 5B-3R). This method has gained popularity in recent years in many health care provider settings for the analysis of specific analytes in blood and tissue samples. A solution prepared from gold coated polystyrene beads modified with DNA hairpins served as a blank to negate the effect of nonspecific binding of probe onto the polystyrene surface. To avoid clogging the nozzle set at 70 μm , the sample was diluted 5 times in a PBS buffer before measurement. Depending on the target of interest, excitation sources of 488 nm or 628 nm were selected with their respective emission filters of either HQ530/30 with an LP505 nm filter or HQ670/30. The event

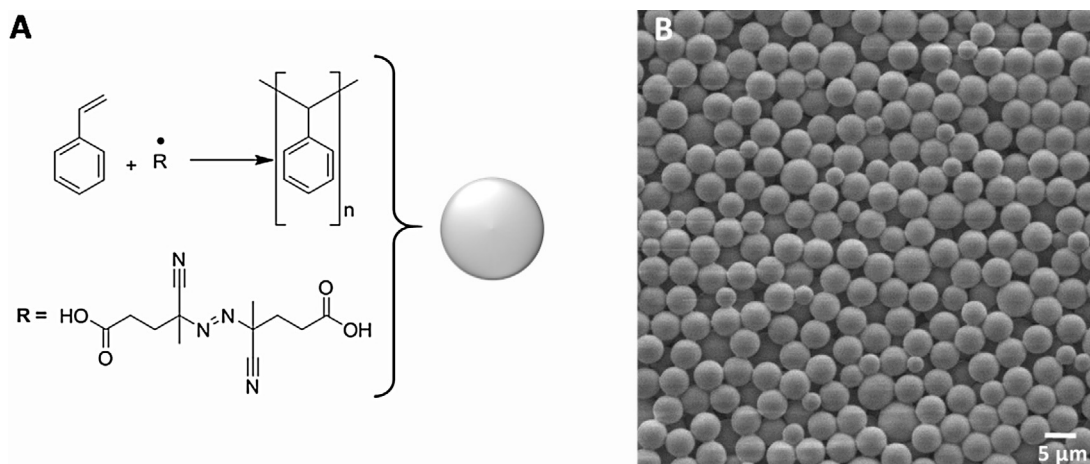


Fig. 2. (A) Dispersion polymerization reaction of polystyrene beads starting from styrene monomer and 4,4'-Azobis(4-cyanovaleric acid) (ACVA) as a free radical initiator. The reaction is performed at 70 °C under inert atmosphere and constant stirring (80 rpm). (B) Scanning electron microscopy image of polystyrene beads prepared at 500:1 monomer:initiator mole ratio. The bead size was analyzed using ImageJ software. Some beads were manually selected for analysis. Average diameter was calculated to be 4.72 μm with standard deviation of 0.48 ($N=235$).

counting was stopped after reaching 10,000 events. The voltages used for the detectors and excitation sources were kept constant throughout the experiment.

4. Results and discussion

In what follows, we will report on the development of a sensing platform that will combine strategies from the field of fluorescence sensing based on metal quenching [44], molecular beacon based on DNA hairpins [34], surface nano-structuring [45,46] and flow cytometry to assemble a sensitive and specific sensor with multiplexing capabilities.

4.1. Characterization of polystyrene gold coated microbeads

In a flow cytometry experiment, scattered light by microparticles is first identified which triggers the detection of a fluorescent signal. It is routinely used to access sub-cell populations expressing different concentrations of fluorescently labeled proteins in cells [47,48]. DNA hairpins assembled on gold nanoparticles are small structures unable to scatter light efficiently to be detected by the flow cytometer (Fig. S1). Micro-sized polystyrene beads (PS) scatter light efficiently and will be used for this purpose in these experiments [49]. The beads need to be large enough to scatter light while remaining suspended in solution. We argued that an average particle diameter between 4 and 6 μm will satisfy these conditions.

The polystyrene beads size is controlled by the initial monomer and initiator concentration [38–40]. The temperature of the reaction vessel and the stirring speed along with the solvent plays a critical role in the beads monodispersity [39,40]. Couple of experimental conditions were tested (Figs. S2 and S3) and as a result, we settled at approximately 500:1 monomer: initiator mole ratio and methoxyethanol, as the solvent of choice. The synthesized beads were characterized using scanning electron microscope, after couple of washing steps (Fig. 2B). The beads average diameter was calculated to be 4.72 μm with a standard deviation of 0.48 μm ($N=235$) (Fig. S4).

In the area of biosensing, introducing nanostructuring patterns improves the sensing properties of the material by increasing the surface area and consequently increasing the available binding sites. In addition, especially in the case of oligonucleotide detection, it increases the accessibility of the target to the surface-immobilized probes [45,43]. Mirkin et al. explored the curvature

effect of spherical gold nanoparticles on the loading density of DNA probes [46]. They reported a critical nanoparticle size in the 60–80 nm range above which the accessibility to the probe is comparable to a planar surface.

As such, polystyrene beads were decorated with small gold nanoparticles (PS-Au) [50]. The nanoparticles serve two essential functions: (i) it will allow the assembly of the nucleotide onto the beads but most importantly, (ii) it will induce the quenching of the fluorescent dye in the absence of the target [35]. Using sodium citrate as a reducing agent, gold nanoparticles were grown onto the polystyrene bead surface and imaged using SEM (Fig. 3A) [50]. The images revealed no change in the size or shape of the polystyrene beads and the successful growth of gold nanoparticles with an average size of 24.7 nm (± 14.3 nm; $N=729$) (Figs. 3B, S5 and S6.A). The large standard deviation could be attributed to the presence of gold nanoparticle islands which were difficult to eliminate. Before reducing the gold nanoparticles on the surface, the polystyrene beads are treated with a mixture of water and ethanol to etch excess PVP of the surface and create sites for the gold to nucleate. This random process might compromise the homogeneity of the gold coating. Another potential route for the formation of these islands might be the large gold nanoparticles that grow in solutions (Fig. S7) which could fuse with the nanoparticles on the polystyrene beads.

The prepared gold particles are below the critical diameter (60–80 nm) and would therefore favor the access of the short oligonucleotide targets to the surface modified hairpin. Elemental analysis also supported the presence of the gold nanoparticles on the PS bead surface (Fig. S6.B).

4.2. Probe loading on the decorated bead particles

The sensor sensitivity greatly depends on the density of the immobilized hairpin on the gold nanoparticle surface [51,52]; the proper folding of the DNA into a closed stem-loop structure is critical to achieve efficient fluorescent quenching and subsequently good signal-to-background ratio upon hybridization of the target of interest. At low surface coverage, the majority of the hairpins, driven by nonspecific adsorption, are surface bound. With the increase of the probe density, steric and electrostatic repulsion inhibit surface adsorption and destabilizes the hairpin formation. To this end, we varied the ratio of PS-Au decorated beads to that of the probe and compared it to unmodified beads (Fig. S8). At the

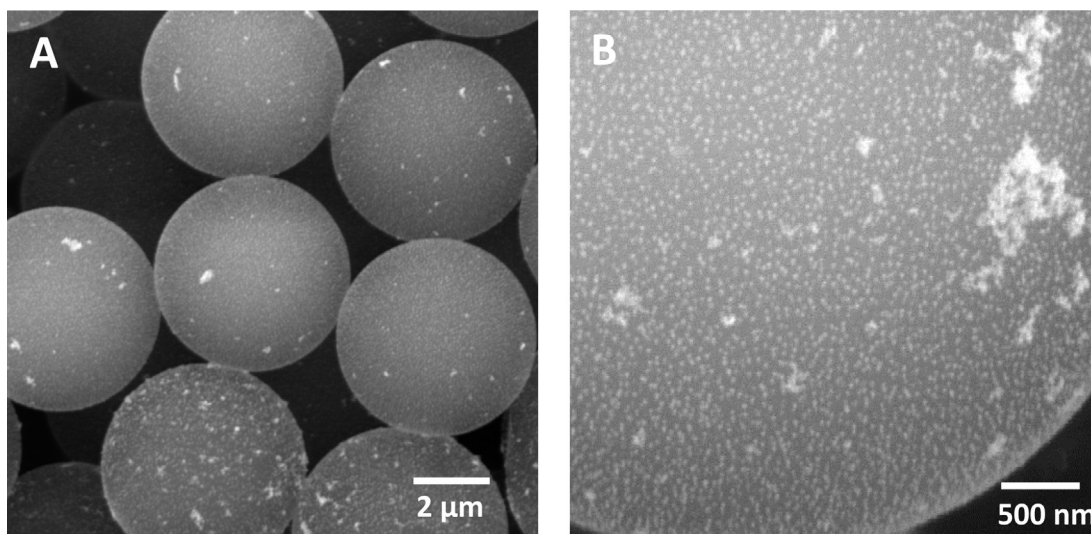


Fig. 3. (A and B) SEM images of gold coated polystyrene beads (PS-Au). The particle size analysis of gold nanoparticles on the surface of a PS bead showed an average diameter was calculated to be equal to 24.74 nm with a standard deviation of 14.36 nm ($N = 729$).

lowest probe/PS beads ratio, a slight increase in the fluorescent signal is recorded (ca. 24) when compared to unmodified beads (ca. 13). When doubling the probe concentration, no major increase in the fluorescent signal is observed. A further increase in the probe concentration led to a jump in the fluorescent signal (ca. 82). We believe that in the lowest two tested ratios the probe is properly folded and the fluorescent dye is in close proximity to the gold surface. Efficient signal suppression is therefore observed. Overcrowding the metal surface would result in unfolding the hairpin and a recovery in the fluorescent signal [52]. Our results are consistent with previously reported studies on DNA hairpins modified gold microelectrodes [51]. In addition, Cederquist et al. showed that the number of bound target dramatically decreases when the probe metal surface density is high [51]. As such, 50 nM of fluorescently labeled DNA hairpins will be combined with a solution of $1 \times$ as prepared solution of polystyrene gold coated microbeads in all the sensing experiments that follow (see Supporting info section IV for detailed calculations).

4.3. Optimizing assay time: salting and hybridization

In the design of any biosensing platform, time is a critical component. Oligonucleotide assembly of packed structures onto gold surface is a time consuming process. Once the probe is added, salt is used to stabilize the hairpin structures by preventing electrostatic repulsions between adjacent strands [42]. However, at high ionic strength, the DNA hairpin is poorly folded [51]. Hurst et al. optimized the DNA loading as a function of the salt concentration. The protocol, as reported, required 4–5 h of preparation with an overnight incubation [53].

The time was long in the context of achieving fast diagnosis. We therefore introduced slight modifications; the sodium chloride concentration was increased from 0.10 M to 0.15 M per increment to achieve a final salt concentration of 0.60 M and we skipped the overnight incubation. The salting time is subsequently reduced to 1 hour with no difference between the recovered detectable fluorescent signals of the two methods (Fig. S10). After addressing the surface density of the DNA hairpins and its loading time, we focused on optimizing the hybridization, another critical time consuming parameter. Typical previously reported numbers ranged between few hours and 24 h [42]. An overnight incubation was eliminated since it limits the range of applications for quick and efficient detections. Times between 10 min and 3 h were tested and showed that

as little as 30 min were enough to get a comparable fluorescent signals to the longer incubation times (Fig. S12). As such, the probe preparation is reduced to one hour of DNA assembly and 30 min of incubation with the target.

4.4. Parallel detection of two specific genomic sequences

To showcase the potential of our sensing platform, we will detect, as a proof of principle, two sequences which each recognize unique regions of the Vaccinia virus (VV) and hepatitis B virus (HBV) genome [54]. The two viruses present a serious threat to the global health problem and their identification is therefore of a great importance [55,56].

Fluorescently labeled DNA hairpins were therefore carefully designed; the complementary sequence to the target was embedded in the loop of the DNA hairpin allowing maximum solution exposure. On either side, it was flanked with complementary nucleotides to fold into the hairpin-loop structure. The stem sequence was designed to have a melting temperature of around 44 °C, assuring the stability of the hairpin structure at room temperature. The probe-target melting temperature was estimated to be around 77 °C in the hybridization buffer. This difference in melting temperature ensures that the hybridized form is the favorable state over the folded quenched structure. The two hairpins were labeled with ATTO 488 and ATTO 647N for HBV and VV, respectively. These fluorophores are spectrally well resolved and will be detected in the FITC (ATTO 488) and APC (ATTO 647N) channels in the flow cytometer.

Decremental amounts of the target were added to the optimized microbeads probe and their recovered fluorescent signal was recorded using a flow cytometer. Both sequences were detected down to a concentration of 5 nM where the mean blank value, assumed to have a Gaussian distribution, and the probe detected signal peak were separated by at least three standard deviations (SD). The detection limit (DL) is marked in Fig. 4 as a red arrow and is calculated from the average and the standard deviation of the blank; $DL = \text{average}_{\text{Blank}} + 3SD_{\text{Blank}}$. When compared to previously reported multiplexing methods, the proposed method has some clear advantages such as easy and fast preparation and shorter assay time. At its current detection limit, the probe is capable of detecting, without the use of PCR, a highly infected individual with HBV [57]. The detection limit is comparable to previously reported results where no enzymatic signal amplification is used.

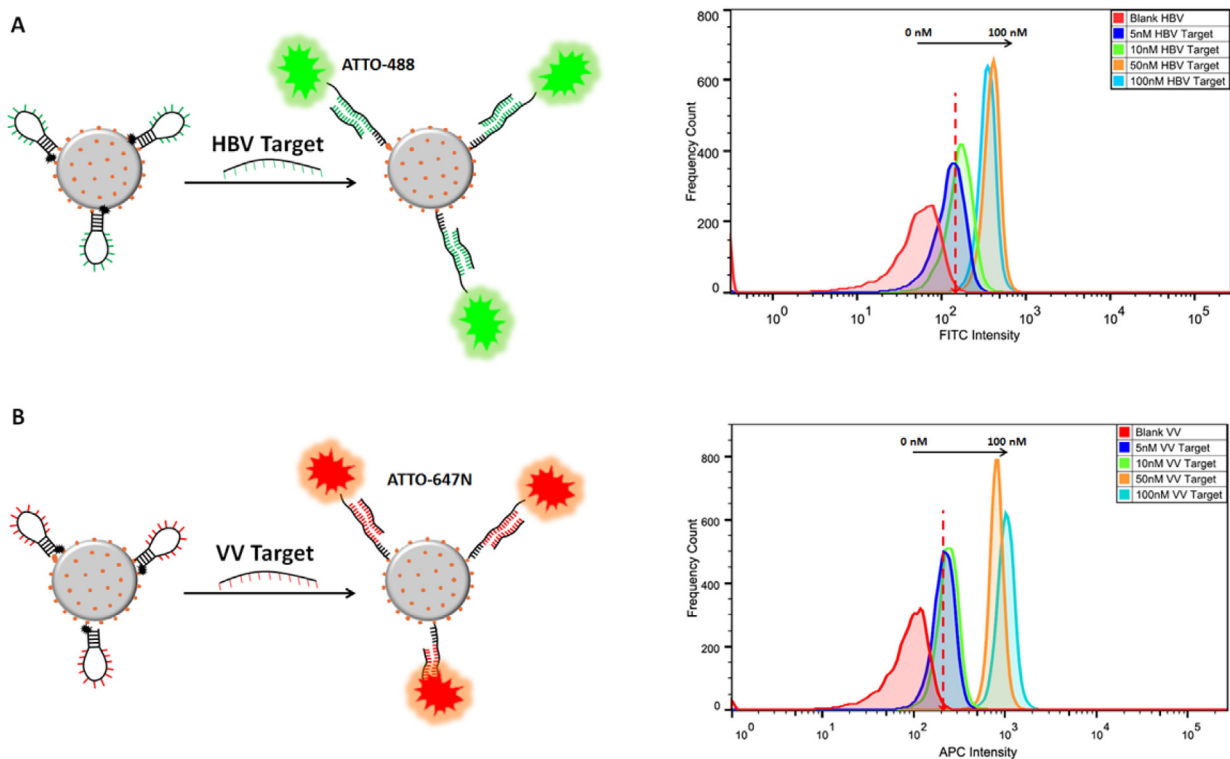


Fig. 4. Titration of different target concentrations (100, 50, 10 and 5 nM) for (A) HBV and (B) VV, independently. Samples were prepared in a hybridization buffer containing 1.8 mM PBS Buffer (pH = 7), NaCl 0.56 M, 2 mM Tris-HCl, 0.4 mM EDTA. Flow cytometer experiments were performed by exciting the samples at 488 nm and recorded in the FITC and APC for HBV and VV, respectively.

Sun et al. reported a fast multiplexing method with a hybridization time of 1 hour and a detection limit of 10 nM for a non-diagnostic oligonucleotide [58]. Zhang et al. also developed a multiplexing fluorescent probe based on silver nanoparticles for the detection of unique genomic sequences for the H1N1 and H5N1. With an incubation time of 24 h, the lowest detection limit was determined to be 25 nM for the two probes [12]. For HBV specifically, Erdem et al. reported an electrochemical method with a reported detection concentration of 10 ppm (equivalent to 2×10^{-5} M) of a 21-mer [59].

Upon closer inspection of the HBV sample, we observed that the detected signal saturates above 50 nM and this also consistent throughout the triplicate trials (Fig. S14). The VV samples, however, did not saturate. We speculate that the HBV probe once folded might be compromising the target accessibility hence the observed saturation. This could be overcome by increasing the number of beads employed in the sensing experiment. The detected fluorescent signal for VV was double than that of HBV. One aspect could be the difference in target accessibility highlighted earlier. Another major factor could be the difference in brightness between the two employed ATTO dyes. The VV probe is labeled with ATTO 647N whose brightness is 1.35 fold greater than that of ATTO 488.

We next focused on the multiplexing capabilities of the prepared microbeads. Quantifying multiple analytes at the same time is now considered a pressing need in the field of medical diagnosis. Flow cytometry presents an advanced and accessible platform which has been used to access sub-fluorescent population for multiplexing experiments [60]. PS beads decorated with both fluorescently labeled HBV and VV probes were mixed with a solution containing 10 nM of HBV, VV or both targets. As shown in Fig. 5, in the presence of only the HBV target, fluorescent signal was detected in the FITC channel with a recorded shift of 185 but none in the APC. The reverse result was obtained in the presence of only VV target (recorded value of 703), while a fluorescent signal was detected

in both channels in the presence of both targets. It is important to point out that the recorded signal intensity was not affected in each channel by the presence of the other fluorescent probe. This multiplexing experiment is also evidence in support of the specificity of the sensing scheme.

4.5. Detection of viral genome in serum

The detection of biomarkers, specifically, circulating oligonucleotides, miRNA in serum is a corner stone in developing point-of-care devices for achieving personalized and preventive medicine. Artificial serum was spiked with 10 and 100 nM VV targets and their detection was compared to that prepared in buffer. As seen in Fig. 6, the target was detected at both low and high concentrations. When compared to the target detected in buffer, no clear difference was observed (Fig. S15).

5. Conclusion

Gold coated microbeads were prepared and used as a platform for the detection of specific viral oligonucleotide sequences in flow cytometric experiments. After tuning the probe density and hybridization time, 5 nM in genetic viral concentration was detected for HBV and VV. The two sequences were detected simultaneously with high specificity in an assay that was optimized to be concluded in less than two hours. VV sequences spiked into artificial serum were detected with the same efficiency as in buffer highlighting the potential of the proposed sensing scheme to transition into a point-of-care device for fast and accurate diagnosis. We believe the reported platform can be applied to detect specific sequences such as miRNAs, circulating oligonucleotides in complex matrices. The Flow cytometry, in particular, can increase the sensitivity and multiplexity capabilities of the sensor. Sample sorting, for instance, when coupled with PCR can dramatically improve

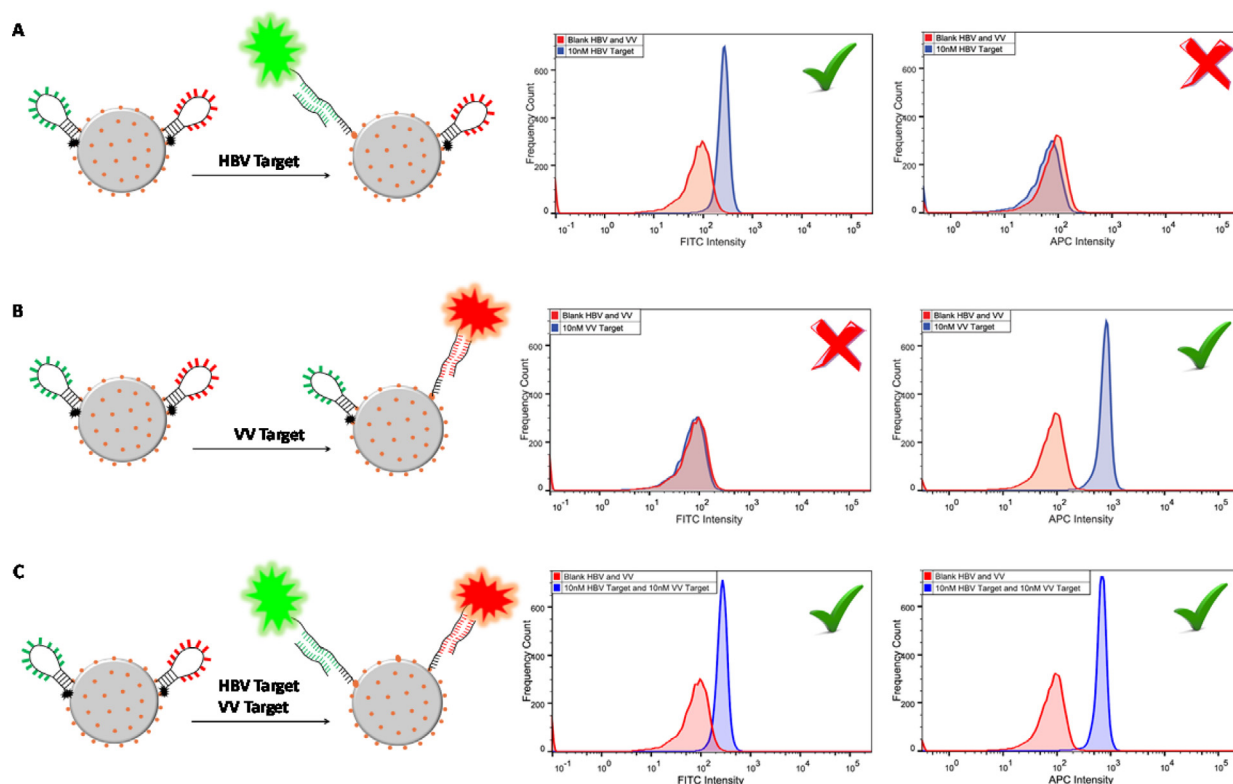


Fig. 5. Flow cytometric measurement of parallel detection of 10 nM (A) HBV, (B) VV, (C) HBV and VV targets when combined with PS-Au beads decorated with both HBV and VV probes.

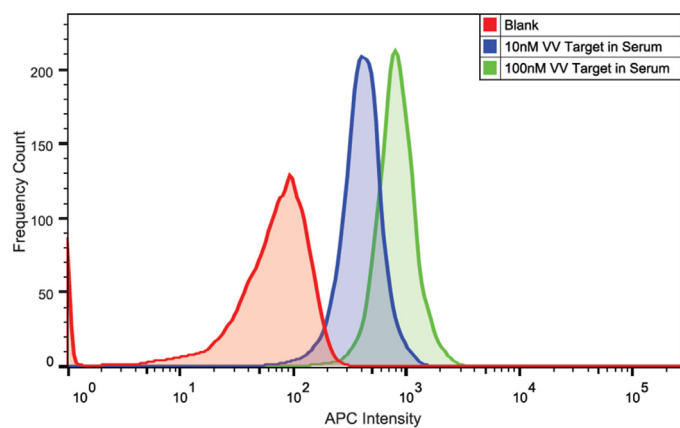


Fig. 6. Flow cytometric measurement of 10 nM and 100 nM VV targets spiked in artificial serum.

the detection limit. Future directions of our work include testing multiple size beads to increase the multiplexing capabilities of our system where subpopulations could be accessed based on not only fluorophore emission but the scattering of the microbeads.

Acknowledgments

This work was supported by the Kamal A. Shair CRSL research fund (# 103191 and # 102998) at the American University of Beirut. The authors are also thankful for the Kamal A. Shair Central Research Science Lab (KAS CRSL) of the Faculty of Arts and Sciences at AUB for providing access to their facilities. H.F. is thankful for the Undergraduate Research Experience Initiative Fund at the American University of Beirut.

Appendix A. Supplementary data

Supplementary data associated with this article can be found, in the online version, at <http://dx.doi.org/10.1016/j.snb.2017.04.066>.

References

- [1] J. Zheng, C. Chen, X. Wang, F. Zhang, P. He, *Sens. Actuators B: Chem.* 199 (2014) 168–174.
- [2] W.W. Ye, J.Y. Shi, C.Y. Chan, Y. Zhang, M. Yang, *Sens. Actuators B: Chem.* 193 (2014) 877–882.
- [3] J. Wang, G. Rivas, X. Cai, E. Palecek, P. Nielsen, H. Shiraishi, N. Dontha, D. Luo, C. Parrado, M. Chicharro, *Anal. Chim. Acta* 347 (1997) 1–8.
- [4] S.R. Paludan, A.G. Bowie, *Immunity* 38 (2013) 870–880.
- [5] M. Ignatiadis, M. Lee, S.S. Jeffrey, *Clin. Cancer Res.* 21 (2015) 4786–4800.
- [6] J. Wang, G. Liu, A. Merkoçi, *J. Am. Chem. Soc.* 125 (2003) 3214–3215.
- [7] K.-J. Huang, Y.-J. Liu, H.-B. Wang, T. Gan, Y.-M. Liu, L.-L. Wang, *Sens. Actuators B: Chem.* 191 (2014) 828–836.
- [8] G. Kocic, G. Bjelakovic, L. Saranac, R. Kocic, T. Jevtic, D. Sokolovic, G. Nikolic, D. Pavlovic, S. Stojanovic, *Diabetes Res. Clin. Pract.* 79 (2008) 204–213.
- [9] F. Wei, P. Patel, W. Liao, K. Chaudhry, L. Zhang, M. Arellano-Garcia, S. Hu, D. Elashoff, H. Zhou, S. Shukla, F. Shah, C.-M. Ho, D.T. Wong, *Clin. Cancer Res.* 15 (2009) 4446–4452.
- [10] P.S. Mitchell, R.K. Parkin, E.M. Kroh, B.R. Fritz, S.K. Wyman, E.L. Pogosova-Agadjanyan, A. Peterson, J. Noteboom, K.C. O'Brian, A. Allen, D.W. Lin, N. Urban, C.W. Drescher, B.S. Knudsen, D.L. Stirewalt, R. Gentleman, R.L. Vessella, P.S. Nelson, D.B. Martin, M. Tewari, *Proc. Natl. Acad. Sci.* 105 (2008) 10513–10518.
- [11] K.P. Porkka, M.J. Pfeiffer, K.K. Waltering, R.L. Vessella, T.L.J. Tammela, T. Visakorpi, *Cancer Res.* 67 (2007) 6130–6135.
- [12] Y. Zhang, C. Zhu, L. Zhang, C. Tan, J. Yang, B. Chen, L. Wang, H. Zhang, *Small* 11 (2015) 1385–1389.
- [13] Y.C. Cao, R. Jin, C.A. Mirkin, *Science* 297 (2002) 1536–1540.
- [14] A. Jemal, R. Siegel, E. Ward, Y. Hao, J. Xu, T. Murray, M.J. Thun, *CA Cancer J. Clin.* 58 (2008) 71–96.
- [15] C. Chen, D.A. Ridzon, A.J. Broomer, Z. Zhou, D.H. Lee, J.T. Nguyen, M. Barbisin, N.L. Xu, V.R. Mahavakar, M.R. Andersen, K.Q. Lao, K.J. Livak, K.J. Guegler, *Nucleic Acids Res.* 33 (2005) e179.
- [16] C.K. Raymond, B.S. Roberts, P. Garrett-Engle, L.P. Lim, J.M. Johnson, *RNA* 11 (2005) 1737–1744.
- [17] Z.-C. Liu, L. Zhang, Y.-M. Zhang, R.-P. Liang, J.-D. Qiu, *Sens. Actuators B: Chem.* 205 (2014) 219–226.

- [18] M. de Planell-Saguer, M.C. Rodicio, Z. Mourelatos, *Nat. Protoc.* 5 (2010) 1061–1073.
- [19] G.J. Nuovo, E.J. Lee, S. Lawler, J. Godlewski, T.D. Schmittgen, *Biotechniques* 46 (2009) 115.
- [20] J.T.G. Pena, C. Sohn-Lee, S.H. Rouhanifard, J. Ludwig, M. Hafner, A. Mihailovic, C. Lim, D. Holoch, P. Berninger, M. Zavolan, T. Tuschl, *Nat. Methods* 6 (2009) 139–141.
- [21] N. Fahlgren, M.D. Howell, K.D. Kasschau, E.J. Chapman, C.M. Sullivan, J.S. Cumbie, S.A. Givan, T.F. Law, S.R. Grant, J.L. Dangl, *PLoS ONE* 2 (2007) e219.
- [22] J. Binladen, M.T.P. Gilbert, J.P. Bollback, F. Panitz, C. Bendixen, R. Nielsen, E. Willerslev, *PLoS ONE* 2 (2007) e197.
- [23] Z. Fang, S.O. Kelley, *Anal. Chem.* 81 (2008) 612–617.
- [24] L. Soleymani, Z. Fang, E.H. Sargent, S.O. Kelley, *Nat. Nano* 4 (2009) 844–848.
- [25] J. Das, K.B. Cederquist, A.A. Zaragoza, P.E. Lee, E.H. Sargent, S.O. Kelley, *Nat. Chem.* 4 (2012) 642–648.
- [26] R. Elghanian, J.J. Storhoff, R.C. Mucic, R.L. Letsinger, C.A. Mirkin, *Science* 277 (1997) 1078–1081.
- [27] M. Han, X. Gao, J.Z. Su, S. Nie, *Nat. Biotechnol.* 19 (2001) 631–635.
- [28] W. Zheng, L. He, J. Am. Chem. Soc. 131 (2009) 3432–3433.
- [29] A.J. Qavi, R.C. Bailey, *Angew. Chem. Int. Ed.* 49 (2010) 4608–4611.
- [30] C.E. Silver, J.J. Beitler, A.R. Shaha, A. Rinaldo, A. Ferlito, *Eur. Arch. Otorhinolaryngol.* 266 (2009) 1333–1352.
- [31] M. Tsujiura, D. Ichikawa, S. Komatsu, A. Shiozaki, H. Takeshita, T. Kosuga, H. Konishi, R. Morimura, K. Deguchi, H. Fujiwara, K. Okamoto, E. Otsuji, *Br. J. Cancer* 102 (2010) 1174–1179.
- [32] Z. Hu, X. Chen, Y. Zhao, T. Tian, G. Jin, Y. Shu, Y. Chen, L. Xu, K. Zen, C. Zhang, H. Shen, *J. Clin. Oncol.* 28 (2010) 1721–1726.
- [33] S. Laing, K. Gracie, K. Faulds, *Chem. Soc. Rev.* 45 (2016) 1901–1918.
- [34] H. Du, M.D. Disney, B.L. Miller, T.D. Krauss, *J. Am. Chem. Soc.* 125 (2003) 4012–4013.
- [35] S. Tyagi, F.R. Kramer, *Nat. Biotechnol.* 14 (1996) 303–308.
- [36] Q. Luan, Y. Xue, X. Yao, *Sens. Actuators B: Chem.* 147 (2010) 561–565.
- [37] H.M. Shapiro, *Practical Flow Cytometry*, John Wiley & Sons, 2005.
- [38] H. Bamnolker, S. Margel, *J. Polym. Sci.* 34 (1996) 1857–1871.
- [39] L. Jinhua, Z. Guangyuan, *Int. J. Polym. Sci.* 2014 (2014) 4.
- [40] A.J. Paine, W. Luymes, J. McNulty, *Macromolecules* 23 (1990) 3104–3109.
- [41] Y. Li, Y. Pan, L. Zhu, Z. Wang, D. Su, G. Xue, *Macromol. Rapid Commun.* 32 (2011) 1741–1747.
- [42] S.J. Hurst, A.K. Lytton-Jean, C.A. Mirkin, *Anal. Chem.* (2006) 8313–8318.
- [43] Y. Cheng, T. Stakenborg, P. Van Dorpe, L. Lagae, M. Wang, H. Chen, G. Borghs, *Anal. Chem.* 83 (2011) 1307–1314.
- [44] H. Du, C.M. Strohsahl, J. Camera, B.L. Miller, T.D. Krauss, *J. Am. Chem. Soc.* 127 (2005) 7932–7940.
- [45] X. Bin, E.H. Sargent, S.O. Kelley, *Anal. Chem.* 82 (2010) 5928–5931.
- [46] H.D. Hill, J.E. Millstone, M.J. Banholzer, C.A. Mirkin, *ACS Nano* 3 (2009) 418–424.
- [47] I. Nicoletti, G. Migliorati, M. Pagliacci, F. Grignani, C. Riccardi, *J. Immunol. Methods* 139 (1991) 271–279.
- [48] S.C. Hur, H.T.K. Tse, D. Di Carlo, *Lab Chip* 10 (2010) 274–280.
- [49] K.L. Kellar, M.A. Iannone, *Exp. Hematol.* 30 (2002) 1227–1237.
- [50] J.-H. Lee, D.O. Kim, G.-S. Song, Y. Lee, S.-B. Jung, J.-D. Nam, *Macromol. Rapid Commun.* 28 (2007) 634–640.
- [51] K.B. Cederquist, R. Stoermer Golightly, C.D. Keating, *Langmuir* 24 (2008) 9162–9171.
- [52] K.B. Cederquist, C.D. Keating, *Langmuir* 26 (2010) 18273–18280.
- [53] C.A. Mirkin, R.L. Letsinger, R.C. Mucic, J.J. Storhoff, *Nature* 382 (1996) 607–609.
- [54] S.I. Stoeva, J.S. Lee, C.S. Thaxton, C.A. Mirkin, *Angew. Chem.* 118 (2006) 3381–3384.
- [55] T.J. Liang, *Hepatology* 49 (2009).
- [56] B.L. Jacobs, J.O. Langland, K.V. Kibler, K.L. Denzler, S.D. White, S.A. Holechek, S. Wong, T. Huynh, C.R. Baskin, *Antiviral Res.* 84 (2009) 1–13.
- [57] S.A. Whalley, J.M. Murray, D. Brown, G.J. Webster, V.C. Emery, G.M. Dusheiko, A.S. Perelson, *J. Exp. Med.* 193 (2001) 847–854.
- [58] S. Sun, H. Yao, F. Zhang, J. Zhu, *Chem. Sci.* 6 (2015) 930–934.
- [59] A. Erdem, K. Kerman, B. Meric, U.S. Akarca, M. Ozsoz, *Anal. Chim. Acta* 422 (2000) 139–149.
- [60] Y. Li, Y.T.H. Cu, D. Luo, *Nat. Biotechnol.* 23 (2005) 885–889.

Biographies

Hassan H. Fakh graduated from the American University of Beirut in 2016 with a Bachelor degree in Chemistry with high distinction. He was the recipient of the Makhlof Haddadin Excellence Award for Undergraduate Senior Student in 2016, and the faculty of Arts and Sciences Undergraduate Research Experience initiative fund. He is currently pursuing his PhD at McGill University.

Malek M. Itani is currently pursuing his Bachelor degree in Chemistry at the American University of Beirut.

Pierre Karam is an assistant professor in the chemistry department at the American University of Beirut. He earned his PhD from McGill University in 2011. Thereafter, he moved to the University of California Berkeley for a postdoctoral position. His research interest is focused on developing biomaterials for sensing applications.